THE JOURNAL OF BIOLOGICAL CHEMISTRY VOL. 288, NO. 2, pp. 1279–1285, January 11, 2013

In Vivo Activation of Azipropofol Prolongs Anesthesia and Reveals Synaptic Targets*

Received for publication, August 27, 2012, and in revised form, November 14, 2012 Published, JBC Papers in Press, November 26, 2012, DOI 10.1074/jbc.M112.413989

Brian P. Weiser[‡§], **Max B. Kelz**[‡¶‖], **and Roderic G. Eckenhoff**[‡1]

From the [‡]*Department of Anesthesia and Critical Care,* [§]*Department of Pharmacology,* [¶]*Center for Sleep and Circadian Neurobiology, and* [‖]*Mahoney Institute of Neurological Sciences, University of Pennsylvania Perelman School of Medicine, Philadelphia, Pennsylvania 19104*

Background: Azipropofol is a photoactive analog of the general anesthetic propofol.
Results: *In vivo* photolabeling of tadpoles results in covalent ligand binding to neuronal proteins and prolongation of anesthesia.
Conclusion: Reconciling time-resolved gel proteomics with behavioral state allows identification of potential anesthetic targets.
Significance: *In vivo* activation of efficacious photolabels provides a novel approach to investigate mechanisms of general anesthesia.

General anesthetic photolabels have been instrumental in discovering and confirming protein binding partners and binding sites of these promiscuous ligands. We report the *in vivo* photoactivation of *meta*-azipropofol, a potent analog of propofol, in *Xenopus laevis* tadpoles. Covalent adduction of *meta*-azipropofol *in vivo* prolongs the primary pharmacologic effect of general anesthetics in a behavioral phenotype we termed "optoanesthesia." Coupling this behavior with a tritiated probe, we performed unbiased, time-resolved gel proteomics to identify neuronal targets of *meta*-azipropofol *in vivo*. We have identified synaptic binding partners, such as synaptosomal-associated protein 25, as well as voltage-dependent anion channels as potential facilitators of the general anesthetic state. Pairing behavioral phenotypes elicited by the activation of efficacious photolabels *in vivo* with time-resolved proteomics provides a novel approach to investigate molecular mechanisms of general anesthetics.

General anesthetics bind many proteins with low affinities (μM K_D values), hindering analyses of ligand-target interactions. Photoactive analogs of clinically used general anesthetics have been developed to aid molecular studies (1–5). These probes share physicochemical properties with their parent molecules, retain anesthetic activity, and undergo photolysis under long wave ultraviolet light (UVA) (315–400 nm), a feature that limits damage to cellular macromolecules upon irradiation following equilibration with the ligands. With these compounds, anesthetic binding sites have been mapped on integrin lymphocyte function-associated antigen (3, 6), *Torpedo* nicotinic receptors (7, 8), β-tubulin (9), PKC (10), and $GABA_A$ receptors (11, 12), among others. Direct identification of anesthetic substrates from complex homogenates has proceeded with a neurosteroid analog (2) and halothane (13), the latter an unaltered general anesthetic containing a carbon-bromine bond broken by shorter UV wavelengths to create reactive carbon-centered radicals (14).

Despite anesthetic efficacy *in vivo*, the use of these probes has been limited to *in vitro* preparations. Electrophysiological evidence supports the concept that covalent incorporation of photoactive anesthetics to binding sites can result in prolonged modulation of functional proteins (15). Although alkylphenol anesthetics are thought to act in part through $GABA_A$ receptors, genetic studies prove that other "on-pathway" targets exist (16, 17). Thus, we tested the feasibility of activating the photoaffinity probe *meta*-azipropofol (AziP*m*)[2] *in vivo* as a tool to identify novel molecular substrates that contribute to alkylphenol general anesthesia. AziP*m* is an analog of propofol (2,6-diisopropylphenol) that contains an alkyl diazirinyl group in the *meta* position of the phenol ring (see Fig. 1) (4). *In vivo* photolabeling of *Xenopus laevis* tadpoles equilibrated with AziP*m* results in a previously unreported behavioral phenotype that we call "optoanesthesia." We describe this in conjunction with unbiased, time-resolved gel proteomics employing a tritiated version of the photolabel.

EXPERIMENTAL PROCEDURES

Materials—2,6-Diisopropylphenol was acquired from Sigma-Aldrich, and AziP*m* was synthesized by W. P. Dailey (University of Pennsylvania) through published methods (4). AziP*m* was radiolabeled by AmBios Labs (Boston, MA) by iodinating the ring and reducing with tritium under catalytic conditions. The final product was purified with HPLC. EcoLite(+) liquid scintillation mixture (MP Biomedicals) was used with a PerkinElmer Life Sciences Tri-Carb 2800TR instrument; a Varian Cary 300 Bio UV-visible spectrophotometer was used for spectroscopy. First and second dimension gels, electrophoresis apparatuses, and molecular weight markers were from Bio-Rad. UVA was generated by filtering a 100-watt arc mercury lamp through colored glass UV-visible broadband (~340–615-nm)

* This work was supported, in whole or in part, by National Institutes of Health Grants GM055876 (to R. G. E.), NS080519 (to B. P. W.), and GM088156 (to M. B. K.).

[1] To whom correspondence should be addressed: Dept. of Anesthesia and Critical Care, University of Pennsylvania Perelman School of Medicine, 3620 Hamilton Walk, Philadelphia, PA. Tel.: 215-662-3705; Fax: 215-349-5078; E-mail: roderic.eckenhoff@uphs.upenn.edu.

[2] The abbreviations used are: AziP*m*, *meta*-azipropofol; IEF, isoelectric focusing; ANOVA, analysis of variance; VDAC, voltage-dependent anion channel.

and UV band-pass (~250–375-nm) filters (lamp and filters from Newport, Stratford, CT). Light intensities (measured with an optical power meter (Thorlabs, Newton, NJ)) were 28.1 microwatts/mm^2 and 27.7 microwatts/mm^2 at 350 and 375 nm, respectively. Albino *X. laevis* tadpoles (stage 45–47) were purchased from Nasco (Fort Atkinson, WI) and housed in supplied pond water for at least 24 h prior to experiments. Animal protocols were approved by the Institutional Animal Care and Use Committee (IACUC) of the University of Pennsylvania.

Tadpole Immobility Studies—Tadpoles were placed in Petri dishes with propofol or AziP*m* dissolved in pond water. The same physicochemical parameters determine anesthetic passage across the gills and skin as does passage across the blood brain barrier (18, 19). In some experiments, after a 30-min equilibration, tadpoles were transferred to fresh water; in others, after equilibration, tadpoles remained on the bench for a sham control or were exposed to UVA (photolabeled *in vivo*) before transfer to fresh water. Immobility was defined (and scored) as the percentage of tadpoles that did not swim, twitch, or right themselves throughout a 30-s time window preceding every 10-min interval. Tadpole assays are established measures of anesthetic potency (18, 19), and reversible immobility is the most commonly used general anesthetic end point. Alternative causes of immobility in our study (*e.g.* muscular toxicity) were not ruled out, but should have had additional and toxic features that would have been observed (*e.g.* cardiac muscle dysfunction, etc). The water temperature was 21–22 °C for experiments and changed <0.5 °C throughout any experiment.

In Vivo Photolabeling and Isolation of Neuronal Membranes—Tadpoles were incubated for 30 min with 4 μM [^{3}H]AziP*m* and treated ± UVA for 10 min. After transfer to fresh water, tricaine methanesulfonate (500 mg/liter) was added immediately for the zero time point or at 165 min for the emergence time point, and the tadpoles were placed on ice. After decapitation, brains and spinal cords were removed with forceps under a dissecting microscope and placed in ice-cold 0.32 M sucrose, 5 mM Tris, pH 7.4, supplemented with protease inhibitors. Tissue isolation required less than 15 min following each time point; central nervous system (CNS) tissue was homogenized every 3–5 min using a Teflon/glass homogenizer.

CNS homogenates were centrifuged at 100,000 × *g* for 10 min, washed with isolation buffer, and recentrifuged. The pellet was homogenized in 5 mM Tris, pH 7.4, and centrifuged at 100,000 × *g* for 10 min, washed, and centrifuged again before resuspension in 2 mM Tris, pH 7.4. An aliquot was removed for a protein assay prior to freezing at −80 °C.

In Vitro Photolabeling—Unexposed tadpoles were anesthetized with tricaine methanesulfonate, and neuronal tissue, dissected as above, was homogenized in sucrose buffer, centrifuged at 100,000 × *g* for 10 min, washed, and recentrifuged. The pellet was suspended in isolation buffer, and the protein concentration was determined and then diluted to 1 mg/ml in a microcentrifuge tube. 4 μM [^{3}H]AziP*m* ± 400 μM propofol was added and, after a brief vortex, the tissue was incubated at 21 °C in the dark for 10 min. After transfer to a quartz cuvette (path length, 1 mm), the tissue was photolabeled for 10 min using the same light source as above. The homogenates were then centrifuged at 100,000 × *g*, homogenized in 5 mM Tris, recentrifuged at 100,000 × *g*, washed, and stored at −80 °C in 2 mM Tris.

Scintillation Counting of Neuronal Tissue—Dissected CNS tissue from tadpoles treated with 4 μM [^{3}H]AziP*m* ± UVA was placed in 1 ml of ice-cold 2% SDS, 1% Triton X-100, 5 mM Tris, pH 7.4, supplemented with protease inhibitors. Following homogenization, the protein concentration was determined. 5 and 10 μl of the homogenates were added to separate vials in scintillation fluid. The disintegrations per minute (dpm) from each vial were normalized to the corresponding protein amount, and the mean of the two values was used for a single experimental measurement.

IEF/SDS-PAGE—After thawing, 100 μg of neuronal membrane protein was centrifuged for 15 min at 15,000 × *g*. Following removal of the supernatant, the pellet was dissolved in 125 μl of 7 M urea, 2 M thiourea, 20 mM dithiothreitol, and 0.2% carrier ampholytes. Isoelectric focusing and SDS-PAGE proceeded according to the manufacturer's instructions, with 3–10 nonlinear pH strips (7 cm) and 4–15% SDS-PAGE. Tissue from ~25 tadpoles sufficed for a single gel.

Spot Intensity Quantitation and Liquid Scintillation Counting—Gels were washed with water and fixed overnight in 15% trichloroacetic acid before staining with Coomassie Blue G-250. After destaining, the gels were scanned on a Bio-Rad GS-800 calibrated densitometer with quantitation performed using the accompanying Quantity One software. Background was subtracted with a box drawn between the 50- and 75- kDa molecular mass markers, and mean optical density multiplied by spot area was recorded from contoured spots.

Spots were excised with a 1.5-mm cylindrical hole punch and placed into scintillation vials. 400 μl of 30% hydrogen peroxide was added, and the sealed vials were incubated overnight at 65 °C to dissolve the polyacrylamide. These were cooled to room temperature before adding scintillation fluid.

Mass Spectrometry Analysis—Trypsin-digested samples were separated on a nanoLC column before online electrospray into a Thermo LTQ linear ion trap. Raw data were acquired with Xcalibur. The National Center for Biotechnology Information (NCBI) online protein database was searched with the term "*Xenopus*," and the FASTA formatted sequences of the results were downloaded. This downloaded database was searched with SEQUEST for protein identification. Parameters were 1 atomic mass unit of parent ion tolerance, 1 atomic mass unit of fragment ion tolerance, and 1 missed cleavage. The search result files were combined with Scaffold 3 and filtered with the following criteria: X_{corr} scores (+1 ion) 1.7, (+2) 2.3, (+3) 2.8; protein identification confidence 99.9%; peptide identification confidence 95%; two peptide minimum. Spectra were manually inspected to ensure quality and confidence.

Statistics—GraphPad Prism 5 was used for figure preparation and data analysis. Student's *t* test, one-way ANOVA, two-way ANOVA, and Bonferroni's correction were calculated within the GraphPad software. Significance is expressed as *, $p < 0.05$ and **, $p < 0.01$.

RESULTS

Optoanesthesia in Xenopus Tadpoles—Albino tadpoles anesthetized with 3 μM propofol or 4 μM AziP*m* (approximate EC_{99}

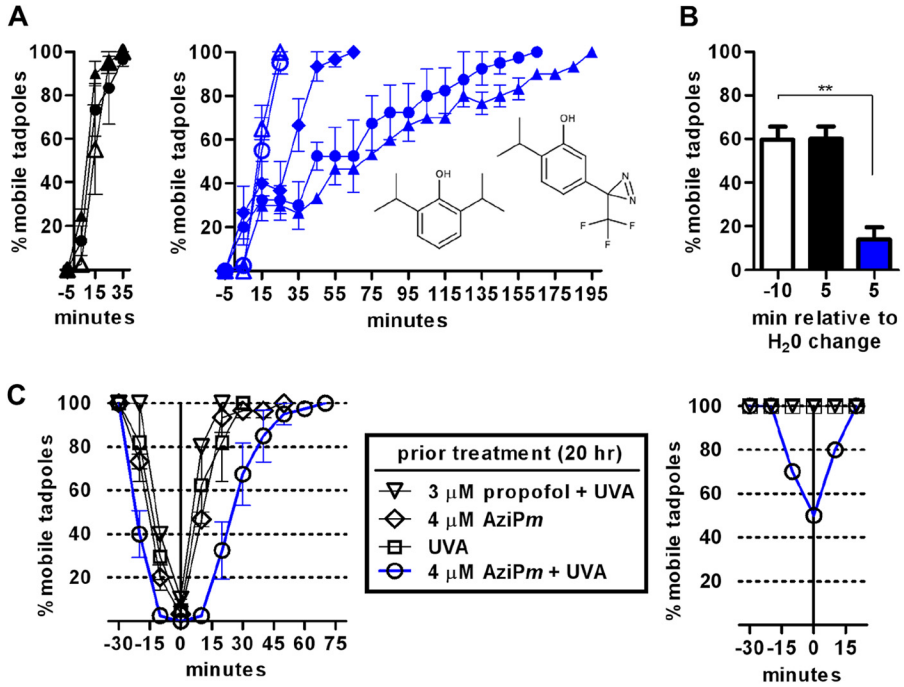

FIGURE 1. *A*, time course of recovery for tadpoles following anesthetic equilibration and (*left*) sham treatment or (*right*) UVA exposure. 3 μM propofol (*open symbols*; *left structure* in *right panel*) or 4 μM AziP*m* (*closed symbols*; *right structure* in *right panel*) was used. Treatment times were 3 min (*diamonds*), 10 min (*circles*), or 20 min (*triangles*), and the water was changed at time 0. Data shown is the mean ± S.E. from 3–4 experiments per group. *B*, *in vivo* photolabeling for 10 min after equilibration with a sub-EC_{99} dose of 3 μM AziP*m* increased the immobile fraction of tadpoles. The water was changed at time 0, with photolabeling from −10 to 0 min. A one-way ANOVA found a significant difference between the three means ($p < 0.01$), and Bonferroni's post hoc test found a significant decrease in the percentage of mobile tadpoles after lamp exposure and water change (*blue bar*, $p < 0.01$). Data represent the mean ± S.E. from three experiments per treatment (± UVA). After equilibration, the tadpoles were randomly assigned to sham or UVA treatment, with the data at −10 min representing both groups and with sham-treated animals represented by the *black bar*. *C*, induction and recovery of tadpoles treated with (*left*) 2 μM propofol or (*right*) 0.8 μM propofol 20 h after the indicated treatments. *Error bars* represent S.E.

doses) recovered on similar time scales following transfer to fresh pond water (Fig. 1*A*, *left*). The tadpoles are equilibrated with the alkylphenol, and recovery under these conditions is largely a function of drug diffusion back into the water.

In this study, we hypothesized that *covalent* occupation of ligand binding sites *in vivo* would result in prolonged anesthetic effects following washout of unadducted compound. The diazirine of AziP*m* has a peak absorbance of ~370 nm, undergoing photolysis to form a reactive carbene, whereas propofol absorbs wavelengths less than 300 nm. Albino tadpoles immobilized with AziP*m* and exposed to UVA before transfer to fresh water exhibited prolonged immobility not observed with propofol control groups (Fig. 1*A*, *right*). Further, a relationship between lamp exposure time and recovery time was evident, suggesting progressive occupancy of functionally relevant sites. No toxicity (premature death) or differences in body mass were observed between tadpoles treated with either alkylphenol anesthetic or alkylphenol anesthetic with UVA following emergence (measured up to 10 days).

Covalent adduction would concentrate ligand into protein sites with infinitely low off-rates, increasing the apparent potency of the molecule. *In vivo* photolabeling for 10 min after equilibration with a sub-EC_{99} AziP*m* dose markedly increased the population of immobilized tadpoles (Fig. 1*B*). Further, we hypothesized that retained attachment of AziP*m* in functionally relevant targets after washout and emergence would manifest as a decrease in the effective concentration of propofol for immobility. Thus, 20 h after emergence, tadpoles treated as above were exposed to 2 or 0.8 μM propofol. Animals photolabeled *in vivo* displayed increased sensitivity (more rapid induction, slower emergence, and induction with a lower dose) relative to controls (Fig. 1*C*).

Lastly, 4 μM AziP*m* in pond water was photolyzed for a period corresponding to twice the diazirine half-life (*i.e.* to a final concentration of ~1 μM (measured by absorption spectroscopy) plus whatever the product(s) of photolysis are). Tadpoles were then placed in this solution, and after 30 min, immobility was not observed, ruling out the possibility that a more potent, "caged" anesthetic with slower washout kinetics was released with light (data not shown). Together, these data suggest prolonged anesthetic influence due to photoadduction of ligand *in vivo*, a phenomenon we termed optoanesthesia.

[^{3}H]AziPm in Tadpole Neuronal Tissue—Because general anesthetics are assumed to exert their effects through CNS targets, retention of photoactivated AziP*m* in neural tissue was measured following optoanesthesia. Brains and spinal cords from control tadpoles and those photolabeled *in vivo* with [^{3}H]AziP*m* were isolated to quantify radioactivity after recovery in fresh water (Fig. 2*A*). Following [^{3}H]AziP*m* induction, without washout, no difference is seen between groups treated ± UVA. However, 8-fold more radioactivity was noted in the neuronal tissue of photolabeled animals at 165 min, the point of emergence for all tadpoles exposed to 4 μM AziP*m* and 10 min of UVA.

Identification of Photolabeled Proteins—Optoanesthesia indicates that neuronal substrates photolabeled *in vivo* are rel-

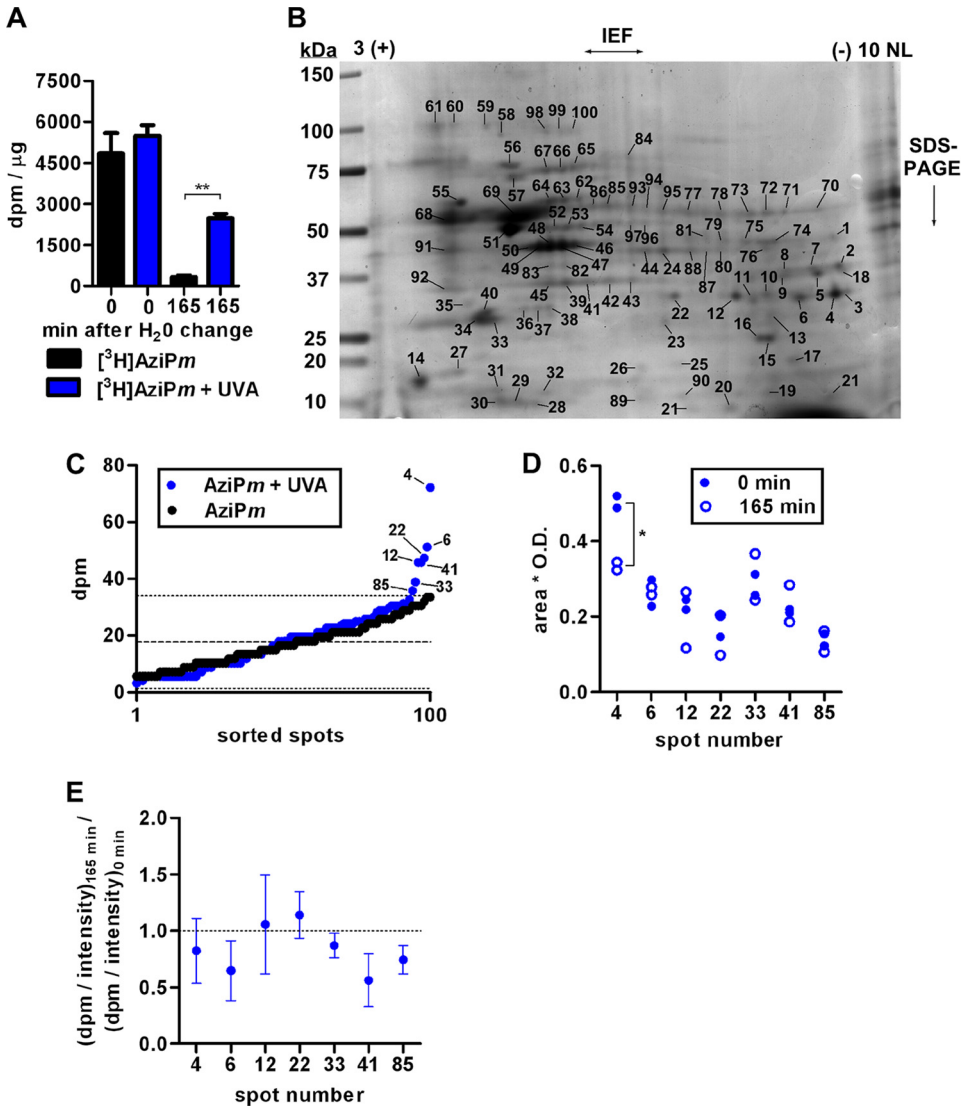

FIGURE 2. *A*, quantitation of dpm normalized to protein amount in CNS tissue of tadpoles treated with AziP*m* ± UVA for 10 min. Data are from 3 experiments per treatment (10 tadpoles per experiment). Mean ± S.E. is shown, and data were analyzed by one-way ANOVA with Bonferroni's post hoc test comparing dpm within each time point ($p < 0.01$). *B*, representative Coomassie Blue-stained gel of tadpole neuronal membrane protein separated first by isoelectric focusing on a 3–10 non-linear (*NL*) pH gradient strip followed by SDS-PAGE. *C*, mean dpm of spots excised from gels of tissue isolated immediately after *in vivo* [^{3}H]AziP*m* ± UVA treatment. dpm values were arranged in ascending order, with measurements from select spots indicated. The *dashed line* indicates background mean from + UVA gels with the *dotted line* indicating two standard deviations. *D*, Coomassie Blue stain intensity quantified from *in vivo* gel spots. Spot 4 was found to decrease with a two-tailed Student's *t* test ($p < 0.05$). *E*, the ratio $(dpm/intensity)_{165\ min}$ divided by $(dpm/intensity)_{0\ min}$ shows the change in the fraction of photolabeled protein over the emergence period. S.D. is shown, and a ratio of 1 would indicate no change.

evant targets of AziP*m* and possibly propofol anesthesia. For protein identifications, neuronal membrane protein from tadpoles equilibrated with [^{3}H]AziP*m* and photolabeled for 10 min was subjected to IEF/SDS-PAGE. Duplicate gels were stained, and 100 random spots were excised for scintillation counting (Fig. 2*B*). Mean background radiation (from three spots excised from each gel containing no detectable Coomassie Blue staining in a region through which the SDS-PAGE separated proteins migrated) was 18.0 dpm, and the mean for all 100 spots was 18.8 dpm. Seven spots contained dpm greater than two standard deviations from the background mean (Fig. 2*C*). No protein spots from control tadpoles incubated with [^{3}H]AziP*m* but not exposed to the lamp contained counts exceeding this background threshold.

Response to in Vivo Photolabeling—We hypothesized that for tadpoles to regain movement ("emerge"), the cellular components contributing to mobility must adapt by removing photolabeled proteins whose activity is altered and/or by replacing these photolabeled macromolecules with newly synthesized proteins. To test this, neuronal membranes were isolated 165 min after tadpoles were photolabeled (when all had emerged) as above for IEF/SDS-PAGE, with the previously identified spots from duplicate gels assayed for dpm. The mean from three spots contained counts within 10% of the initial value (12, 22, and 33), whereas decreases of 46, 35, 42, and 28% were noted in spots 4, 6, 41, and 85, respectively. Coomassie Blue intensity was quantified to assess changes in protein expression, and with the exception of spot 4, little variation was observed (Fig. 2*D*).

Spot dpm was normalized to corresponding Coomassie Blue intensities for the *in vivo* experiments. We proposed that proteins with decreased radioactivity content coincident with emergence gain additional credibility as functionally important

TABLE 1
Protein spot analysis and LC-MS/MS identification

Spot	% of displacement[a]	Protein ID	NCBI accession number	Theoretical[b] molecular mass	Observed[c] molecular mass	Theoretical[b] pI	Observed[c] pI	% of sequence coverage	Spectra count
				Da	*Da*				
4	40.1	VDAC-2	gi 62826006	30,183	27,937	8.36	8.99	29	18
6	52.0	VDAC-2	gi 62826006	30,183	27,448	8.36	8.27	23	14
12	46.5	VDAC-1	gi 28302268	30,627	28,671	6.85	6.71	20	11
22	74.5	VDAC-1	gi 28302268	30,627	29,160	6.85	6.21	26	16
33	3.4	SNAP-25	gi 33416802	23,172	26,468	4.74	4.89	30	15
41	1.7	$G\beta_4$	gi 49257618	37,504	33,084	5.70	5.78	20	11
85	26.6	PDIA3	gi 28302197	56,086	54,992	5.72	5.91	30	25
	26.6	VHA-55	gi 28436920	56,411	54,992	5.56	5.91	20	21

[a] [^{3}H]AziP*m* displacement by propofol from in vitro photolabeling experiments.
[b] Theoretical values were computed with the ExPASy Compute pI/Mw tool. Monoisotopic molecular weights are shown.
[c] Observed values were estimated from molecular weight markers and IEF-resolving estimations published by the manufacturer of the gels.

targets. Thus, we calculated the *ratio* of normalized photolabel incorporation at 165 min to that at the zero time point for each spot (Fig. 2*E*). A ratio of 1 would indicate that the fraction of adducted protein did not change over the 165 min. We found that the ratios from spots 6, 33, 41, and 85 are significantly less than 1, suggesting potential relevance in emergence from optoanesthesia.

Conserved Specificity and Target Identification—In vitro photolabeling of neuronal homogenates with 4 μM [^{3}H]AziP*m* ± 400 μM propofol was performed to investigate the conserved, saturable specificity of protein sites. Protein spots identified as photolabeled *in vivo* were analyzed, and all contained dpm above background. A significant effect of propofol on normalized dpm was revealed with decreased photolabel incorporation ranging from 2 to 75% in each spot ($p < 0.05$, two-way ANOVA; $n = 3$ and $n = 2$ for each spot (−) and (+) propofol, respectively) (Table 1). A separate gel was run for protein identification. Six spots were unambiguously identified as containing a single protein, whereas two high confidence identifications were possible in the seventh (Table 1).

DISCUSSION

We describe optoanesthesia, a light-induced anesthetic potentiation, and present a method through which novel general anesthetic targets can be discovered. Reconciling proteomic data with a behavioral phenotype provides a powerful means to assign relevance to identified binding partners. The mechanisms of recovery from optoanesthesia are likely to reside in adducted, relevant proteins being targeted for accelerated degradation and/or being replaced by newly synthesized protein. An alternative hypothesis, not tested here, is that the activities of proteins that are not targets of AziP*m* are altered to compensate for the covalent modification of the alkylphenol binding partners. Although emergence pathways may be distinct from induction pathways (20), emergence must still require an offloading of the anesthetic from induction targets; thus, we view our initial hypothesis, that label intensity should decrease in functionally relevant targets, as reasonable.

Performing photolabeling in live organisms assured that molecular targets were in a functional state, and because the primary effect of the anesthetic (immobility) was prolonged, confirmed that relevant targets were adducted. Further evidence for ligand incorporation to relevant general anesthetic sites was seen by the increased sensitivity to propofol after *in vivo* photolabeling. Despite label attachment to the identical proteins *in vitro*, substantial displacement of photoactive ligand by the parent propofol was most evident with VDACs. These mitochondrial porins with multiple phosphorylation states were also the most prominently labeled proteins *in vivo*. Protection of photolabeling by propofol suggests conserved and specific alkylphenol site(s). An alternative explanation for propofol competition is allosterism, which would require separate specific cavities for AziP*m* and for propofol, a possibility we view as unlikely.

Although VDACs are highly abundant proteins, this binding is not interpreted as "nonspecific." Specificity can be viewed as *specific to a particular physiological outcome* or, on the molecular level (and favored here), *high occupancy, saturable binding*. Other general anesthetics have been shown to bind VDACs *in vitro*, but functional consequences have yet to be reported. VDACs bind $GABA_A$ receptors (21, 22), known propofol targets, but knock-outs of VDAC-1 and VDAC-3 do not appear to alter anesthetic sensitivity (22). Knock-out of VDAC-2 in mice is embryonic lethal, and interestingly, our time-resolved approach implicates VDAC-2 over VDAC-1 and VDAC-3 (Fig. 2*E*). However, this may reflect a general "protective" effect of VDAC-2 from cellular apoptosis (23).

Of the other identified proteins, SNAP-25 and $G\beta_4$ exhibited decreases in the ratio of photolabeled to unmodified protein at the time of emergence. Published evidence has suggested that anesthetic interactions with SNAP-25 and/or $G\beta_4$ might contribute to depressed neuronal signaling. For example, SNAP-25, a component of the ternary SNARE complex, binds volatile anesthetics at physiologically relevant concentrations (24), and isoflurane and propofol inhibit neurotransmitter release through interactions with SNAREs or associated proteins (25, 26). Mutagenesis in SNARE complex proteins (including SNAP-25) alters organism sensitivity to general anesthetics (27). Mammalian studies suggest that SNAP-25 may be predominantly expressed in excitatory neurons (28, 29), and this protein negatively regulates voltage-gated calcium channels independent of its role in exocytosis (30, 31). $G\beta$ (as part of $G\beta\gamma$) can also directly inhibit presynaptic voltage-gated calcium channels (32, 33) and binds to SNAP-25 and syntaxin to inhibit neuronal exocytosis (34, 35).

The lack of [^{3}H]AziP*m* displacement by propofol on some proteins can be interpreted in several ways. For instance, anes-

thetic site(s) (*e.g.* on SNAREs) may not be conserved among ligands; isoflurane and halothane bind to the SNARE complex in a noncompetitive and nonsaturable manner (24). The hydrophobic interior of the coiled-coil complex likely harbors multiple sites of varying affinities, each capable of binding ligands with low occupancy. Alternatively, protein substrates (including Gβ) may be specific to AziP*m* but not propofol (propofol specificity was tested as the photolabel parent). Regardless, these interpretations do not preclude functional involvement in hypnosis or optoanesthesia, as we did not test competition with nontritiated AziP*m*, but also, little evidence suggests that saturable binding underlies these states.

With our approach in a model vertebrate organism, the tadpole, we provide *in vivo* evidence for the functional involvement of synaptic targets previously suspected only from *in vitro* or lower organism studies. Proving this involvement will require extensive genetic manipulations. Additionally, we have identified only a subset of targets bound by AziP*m in vivo*, not including ion channels (such as the $GABA_A$ receptor) that are the object of some general anesthetic hypotheses. Resolving low abundance proteins with multiple transmembrane domains is not feasible with IEF/SDS-PAGE (36, 37), and thus, *a priori* we did not anticipate their identification. The development of proteomic approaches complimentary to IEF/SDS-PAGE, and those that are capable of expanding the dynamic range of neuronal protein detection, will further the investigative power of optoanesthesia.

In conclusion, we anticipate the translation of *in vivo* photolabeling and behavior-paired proteomics to a wider variety of model organisms and photoactive molecules to investigate molecular mechanisms of general anesthetic pharmacology.

Acknowledgments—We thank Bill Dailey for synthesizing meta-azipropofol and Chao-Xing Yuan of the University of Pennsylvania Proteomics Core for assistance with mass spectrometry experiments.

REFERENCES

1. Husain, S. S., Ziebell, M. R., Ruesch, D., Hong, F., Arevalo, E., Kosterlitz, J. A., Olsen, R. W., Forman, S. A., Cohen, J. B., and Miller, K. W. (2003) 2-(3-Methyl-3*H*-diaziren-3-yl)ethyl 1-(1-phenylethyl)-1*H*-imidazole-5-carboxylate: a derivative of the stereoselective general anesthetic etomidate for photolabeling ligand-gated ion channels. *J. Med. Chem.* **46,** 1257–1265
2. Darbandi-Tonkabon, R., Hastings, W. R., Zeng, C.-M., Akk, G., Manion, B. D., Bracamontes, J. R., Steinbach, J. H., Mennerick, S. J., Covey, D. F., and Evers, A. S. (2003) Photoaffinity labeling with a neuroactive steroid analogue: 6-azi-pregnanolone labels voltage-dependent anion channel-1 in rat brain. *J. Biol. Chem.* **278,** 13196–13206
3. Eckenhoff, R. G., Xi, J., Shimaoka, M., Bhattacharji, A., Covarrubias, M., and Dailey, W. P. (2010) Azi-isoflurane, a photolabel analog of the commonly used inhaled general anesthetic isoflurane. *ACS Chem. Neurosci.* **1,** 139–145
4. Hall, M. A., Xi, J., Lor, C., Dai, S., Pearce, R., Dailey, W. P., and Eckenhoff, R. G. (2010) *m*-Azipropofol (AziPm) a photoactive analogue of the intravenous general anesthetic propofol. *J. Med. Chem.* **53,** 5667–5675
5. Stewart, D. S., Savechenkov, P. Y., Dostalova, Z., Chiara, D. C., Ge, R., Raines, D. E., Cohen, J. B., Forman, S. A., Bruzik, K. S., and Miller, K. W. (2011) *p*-(4-Azipentyl)propofol: a potent photoreactive general anesthetic derivative of propofol. *J. Med. Chem.* **54,** 8124–8135
6. Yuki, K., Bu, W., Xi, J., Sen, M., Shimaoka, M., and Eckenhoff, R. G. (2012) Isoflurane binds and stabilizes a closed conformation of the leukocyte function-associated antigen-1. *FASEB J.* **26,** 4408–4417
7. Ziebell, M. R., Nirthanan, S., Husain, S. S., Miller, K. W., and Cohen, J. B. (2004) Identification of binding sites in the nicotinic acetylcholine receptor for [^{3}H]azietomidate, a photoactivatable general anesthetic. *J. Biol. Chem.* **279,** 17640–17649
8. Cui, T., Mowrey, D., Bondarenko, V., Tillman, T., Ma, D., Landrum, E., Perez-Aguilar, J. M., He, J., Wang, W., Saven, J. G., Eckenhoff, R. G., Tang, P., and Xu, Y. (2012) NMR structure and dynamics of a designed water-soluble transmembrane domain of nicotinic acetylcholine receptor. *Biochim. Biophys. Acta* **1818,** 617–626
9. Chen, Z.-W., Chen, L.-H., Akentieva, N., Lichti, C. F., Darbandi, R., Hastings, R., Covey, D. F., Reichert, D. E., Townsend, R. R., and Evers, A. S. (2012) A neurosteroid analogue photolabeling reagent labels the colchicine-binding site on tubulin: a mass spectrometric analysis. *Electrophoresis* **33,** 666–674
10. Das, J., Addona, G. H., Sandberg, W. S., Husain, S. S., Stehle, T., and Miller, K. W. (2004) Identification of a general anesthetic binding site in the diacylglycerol-binding domain of protein kinase Cδ. *J. Biol. Chem.* **279,** 37964–37972
11. Li, G.-D., Chiara, D. C., Sawyer, G. W., Husain, S. S., Olsen, R. W., and Cohen, J. B. (2006) Identification of a $GABA_A$ receptor anesthetic binding site at subunit interfaces by photolabeling with an etomidate analog. *J. Neurosci.* **26,** 11599–11605
12. Chen, Z.-W., Manion, B., Townsend, R. R., Reichert, D. E., Covey, D. F., Steinbach, J. H., Sieghart, W., Fuchs, K., and Evers, A. S. (2012) Neurosteroid analogue photolabeling of a site in the TM3 domain of the β3 subunit of the $GABA_A$ receptor. *Mol. Pharmacol.* **82,** 408–419
13. Xi, J., Liu, R., Asbury, G. R., Eckenhoff, M. F., and Eckenhoff, R. G. (2004) Inhalational anesthetic-binding proteins in rat neuronal membranes. *J. Biol. Chem.* **279,** 19628–19633
14. Eckenhoff, R. G., and Shuman, H. (1993) Halothane binding to soluble proteins determined by photoaffinity labeling. *Anesthesiology* **79,** 96–106
15. Zhong, H., Rüsch, D., and Forman, S. A. (2008) Photo-activated azi-etomidate, a general anesthetic photolabel, irreversibly enhances gating and desensitization of γ-aminobutyric acid type A receptors. *Anesthesiology* **108,** 103–112
16. Jurd, R., Arras, M., Lambert, S., Drexler, B., Siegwart, R., Crestani, F., Zaugg, M., Vogt, K. E., Ledermann, B., Antkowiak, B., and Rudolph, U. (2003) General anesthetic actions *in vivo* strongly attenuated by a point mutation in the $GABA_A$ receptor β3 subunit. *FASEB J.* **17,** 250–252
17. Nguyen, H. T., Li, K. Y., daGraca, R. L., Delphin, E., Xiong, M., and Ye, J. H. (2009) Behavior and cellular evidence for propofol-induced hypnosis involving brain glycine receptors. *Anesthesiology* **110,** 326–332
18. Downes, H., and Courogen, P. M. (1996) Contrasting effects of anesthetics in tadpole bioassays. *J. Pharmacol. Exp. Ther.* **278,** 284–296
19. Krasowski, M. D., Jenkins, A., Flood, P., Kung, A. Y., Hopfinger, A. J., and Harrison, N. L. (2001) General anesthetic potencies of a series of propofol analogs correlate with potency for potentiation of γ-aminobutyric acid (GABA) current at the $GABA_A$ receptor but not with lipid solubility. *J. Pharmacol. Exp. Ther.* **297,** 338–351
20. Friedman, E. B., Sun, Y., Moore, J. T., Hung, H.-T., Meng, Q. C., Perera, P., Joiner, W. J., Thomas, S. A., Eckenhoff, R. G., Sehgal, A., and Kelz, M. B. (2010) A conserved behavioral state barrier impedes transitions between anesthetic-induced unconsciousness and wakefulness: evidence for neural inertia. *PLoS One* **5,** e11903
21. Bureau, M. H., Khrestchatisky, M., Heeren, M. A., Zambrowicz, E. B., Kim, H., Grisar, T. M., Colombini, M., Tobin, A. J., and Olsen, R. W. (1992) Isolation and cloning of a voltage-dependent anion channel-like M_r 36,000 polypeptide from mammalian brain. *J. Biol. Chem.* **267,** 8679–8684
22. Darbandi-Tonkabon, R., Manion, B. D., Hastings, W. R., Craigen, W. J., Akk, G., Bracamontes, J. R., He, Y., Sheiko, T. V., Steinbach, J. H., Mennerick, S. J., Covey, D. F., and Evers, A. S. (2004) Neuroactive steroid interactions with voltage-dependent anion channels: lack of relationship to $GABA_A$ receptor modulation and anesthesia. *J. Pharmacol. Exp. Ther.* **308,** 502–511
23. Cheng, E. H. Y., Sheiko, T. V., Fisher, J. K., Craigen, W. J., and Korsmeyer, S. J. (2003) VDAC2 inhibits BAK activation and mitochondrial apoptosis. *Science* **301,** 513–517

24. Nagele, P., Mendel, J. B., Placzek, W. J., Scott, B. A., D'Avignon, D. A., and Crowder, C. M. (2005) Volatile anesthetics bind rat synaptic snare proteins. *Anesthesiology* **103,** 768–778
25. Herring, B. E., Xie, Z., Marks, J., and Fox, A. P. (2009) Isoflurane inhibits the neurotransmitter release machinery. *J. Neurophysiol.* **102,** 1265–1273
26. Herring, B. E., McMillan, K., Pike, C. M., Marks, J., Fox, A. P., and Xie, Z. (2011) Etomidate and propofol inhibit the neurotransmitter release machinery at different sites. *J. Physiol.* **589,** 1103–1115
27. van Swinderen, B., Saifee, O., Shebester, L., Roberson, R., Nonet, M. L., and Crowder, C. M. (1999) A neomorphic syntaxin mutation blocks volatile-anesthetic action in *Caenorhabditis elegans*. *Proc. Natl. Acad. Sci. U.S.A.* **96,** 2479–2484
28. Verderio, C., Pozzi, D., Pravettoni, E., Inverardi, F., Schenk, U., Coco, S., Proux-Gillardeaux, V., Galli, T., Rossetto, O., Frassoni, C., and Matteoli, M. (2004) SNAP-25 modulation of calcium dynamics underlies differences in GABAergic and glutamatergic responsiveness to depolarization. *Neuron* **41,** 599–610
29. Garbelli, R., Inverardi, F., Medici, V., Amadeo, A., Verderio, C., Matteoli, M., and Frassoni, C. (2008) Heterogeneous expression of SNAP-25 in rat and human brain. *J. Comp. Neurol.* **506,** 373–386
30. Wiser, O., Trus, M., Hernández, A., Renström, E., Barg, S., Rorsman, P., and Atlas, D. (1999) The voltage sensitive Lc-type Ca^{2+} channel is functionally coupled to the exocytotic machinery. *Proc. Natl. Acad. Sci. U.S.A.* **96,** 248–253
31. Condliffe, S. B., Corradini, I., Pozzi, D., Verderio, C., and Matteoli, M. (2010) Endogenous SNAP-25 regulates native voltage-gated calcium channels in glutamatergic neurons. *J. Biol. Chem.* **285,** 24968–24976
32. Ikeda, S. R. (1996) Voltage-dependent modulation of N-type calcium channels by G-protein $\beta\gamma$ subunits. *Nature* **380,** 255–258
33. Herlitze, S., Garcia, D. E., Mackie, K., Hille, B., Scheuer, T., and Catterall, W. A. (1996) Modulation of Ca^{2+} channels by G-protein $\beta\gamma$ subunits. *Nature* **380,** 258–262
34. Gerachshenko, T., Blackmer, T., Yoon, E.-J., Bartleson, C., Hamm, H. E., and Alford, S. (2005) G$\beta\gamma$ acts at the C terminus of SNAP-25 to mediate presynaptic inhibition. *Nat. Neurosci.* **8,** 597–605
35. Blackmer, T., Larsen, E. C., Bartleson, C., Kowalchyk, J. A., Yoon, E.-J., Preininger, A. M., Alford, S., Hamm, H. E., and Martin, T. F. J. (2005) G protein $\beta\gamma$ directly regulates SNARE protein fusion machinery for secretory granule exocytosis. *Nat. Neurosci.* **8,** 421–425
36. Bunai, K., and Yamane, K. (2005) Effectiveness and limitation of two-dimensional gel electrophoresis in bacterial membrane protein proteomics and perspectives. *J. Chromatogr. B Analyt. Technol. Biomed. Life Sci.* **815,** 227–236
37. Issaq, H., and Veenstra, T. (2008) Two-dimensional polyacrylamide gel electrophoresis (2D-PAGE): advances and perspectives. *BioTechniques* **44,** 697–698, 700